CLNS 01/1754

Active cooling control of the CLEO detector using a hydrocarbon coolant farm

A. Warburton [a,*], K. Arndt [b], C. Bebek [a,1], J. Cherwinka [a,2], D. Cinabro [c], J. Fast [b,3], B. Gittelman [a], Seung J. Lee [a], S. McGee [c], M. Palmer [a], L. Perera [c,4], A. Smith [d], D. Tournear [b,5], and C. Ward [a,6].

[a] *Wilson Synchrotron, Laboratory of Nuclear Studies, Cornell University, Ithaca, New York 14853, USA*

[b] *Purdue University, West Lafayette, Indiana 47907, USA*

[c] *Wayne State University, Detroit, Michigan 48202, USA*

[d] *University of Minnesota, Minneapolis, Minnesota 55455, USA*

Abstract

We describe a novel approach to particle-detector cooling in which a modular farm of active coolant-control platforms provides independent and regulated heat removal from four recently upgraded subsystems of the CLEO detector: the ring-imaging Čerenkov detector, the drift chamber, the silicon vertex detector, and the beryllium beam pipe. We report on several aspects of the system: the suitability of using the aliphatic-hydrocarbon solvent PF^{TM}-200IG as a heat-transfer fluid, the sensor elements and the mechanical design of the farm platforms, a control system that is founded upon a commercial programmable logic controller employed in industrial process-control applications, and a diagnostic system based on virtual instrumentation. We summarize the system's performance and point out the potential application of the design to future high-energy physics apparatus.

Key words: CLEO, Detector, Cooling, Process Control, Hydrocarbon Heat-Transfer Fluids
PACS: 29.90.+r, 07.07.−a, 07.05.Dz, 65.20.+w

Article published in Nuclear Instruments and Methods in Physics Research A

1 CLEO experiment

The CLEO experiment, located on the Cornell Electron Storage Ring (CESR), consists of a general-purpose particle physics detector [1,2] used to reconstruct the products of symmetric e^+e^- collisions with centre-of-mass energies up to approximately 10 GeV, corresponding to the $\Upsilon(4S)$ resonance. Luminosity-increasing improvements in the CESR optics, which required the placement of superconducting quadrupole magnets nearer to the e^+e^- interaction region, precipitated upgrades to several inner subsystems of the detector prior to the CLEO III datataking run.

The main outer components of the CLEO detector are a CsI electromagnetic calorimeter, a 1.5 T solenoidal superconducting magnet, and muon detectors. The upgraded inner subsystems consist of, in order of decreasing radius with respect to the e^+e^- beam line, the following four devices: a 230 400 channel ring-imaging Čerenkov (RICH) detector for charged-hadron identification [3]; a new central drift chamber [4], with 9796 cells arranged in 47 layers, for charged-particle tracking; a four-layer double-sided silicon microstrip vertex detector [5] with 125 000 readout channels for precise tracking and decay vertexing; and a thinly walled beryllium beam pipe [6] to minimize tracking uncertainties due to multiple-scattering effects.

An active coolant-control farm, which is the focus of this article, was used to provide heat removal and mechanical stability (via temperature control) for the above four upgraded inner CLEO subsystems. In the case of the RICH detector, the principal heat sources were chains of Viking [7] front-end signal processing chips, with a combined power output of ∼360 W. The drift chamber's heat sources consisted of a total of ∼150 W of power dissipated by pre-amplifiers mounted on each of the two end plates; temperature stability across the end plates was crucial to prevent wire breakage. The silicon detector produced ∼488 W of power from 122 BeO hybrid boards of front-end electronics chips [8], each dissipating 4 W; spatial tracking resolution of the silicon layers depended on the alignment precision of the sensors and therefore the temperature stability. The Be beam pipe was itself passive, but required a de-

* Corresponding author.
Email address: AndreasWarburton@mailaps.org (A. Warburton).
[1] Current address: Lawrence Berkeley National Laboratory, Berkeley, California 94720, USA.
[2] Current address: Focused Research, Inc., Middleton, Wisconsin 53562, USA.
[3] Current address: Fermi National Accelerator Laboratory, Batavia, Illinois 60510, USA.
[4] Current address: Rutgers University, Piscataway, New Jersey 08855, USA.
[5] Current address: Stanford University, Stanford, California 94305, USA.
[6] Current address: Intel Corporation, Hillsboro, Oregon 97124, USA.

sign heat-removal capability up to the $0.5-1$ kW range due to the possibility of higher-order mode heating in the CESR e^+e^- collider.

In this article, we describe the approach taken in designing the CLEO coolant-control farm, studies of the hydrocarbon PF$^{\mathrm{TM}}$-200IG and its suitability as a heat-transfer fluid, mechanical construction of the farm platforms, the sensor elements, the process-control and diagnostic systems, and the farm's performance in the CLEO III datataking run.

2 Design approach

2.1 Generality, scalability, and modularity

The principal challenge posed in the design of the CLEO cooling system lay in the requirement that multiple detector subsystems, each with markedly different plumbing layouts, power loads, pressure tolerances, and physical locations, were to be actively cooled by a 'farm' of independent coolant-control platforms governed and monitored by centralized control and diagnostic systems, respectively. Rather than design separate custom coolant circuits tailored to the specifications of each detector subsystem, our approach was to found the system on a single simple generic design, one that possessed the flexibility to satisfy the cooling requirements of any of the subsystems without extensive modification.

The advantages of a scalable generic design were numerous. Each system had the same basic set of fittings and sensors, introducing economies of scale and easing spare-component inventories. The modularity of the design was intended to allow for the rapid swapping of an entire coolant-control platform with a spare unit in case of a problem. The offending platform could then be removed *en masse* from the radiation area for diagnosis and repair, without the accrual of excessive downtime. Technician training, serviceability, and the management of on-call experts were simpler in this farm paradigm; separate cooling experts were not required for different detector subsystems, and the total number of experts needed was reduced.

Our use of a modular farm of nearly identical cooling platforms lent itself well to a unified process-control system, which we describe in Section 6. Scaling of the control electronics to accommodate additional coolant platforms was designed to be a facile matter of adding more input/output channels and updating the control logic. All electronic sensors, including those not used for process-control variables, were read out by the control electronics. A separate diagnostic system, described in Section 7, therefore had no need to in-

teract with the farm sensors directly; instead, all the diagnostic information was acquired through the control infrastructure. The diagnostic system was designed to provide globally accessible, minute-by-minute performance information browsable on the World Wide Web (WWW).

Beneficial to the farm concept was a simple, rapid, and independent channel of communication between the coolant-control electronics and the detector subsystems proper. Instead of using a subsystem-based temperature reading, which would have required significant customization on each platform, the cooling platforms used the temperatures of their coolant supply as process variables, thereby precluding a need for the detector subsystems to communicate with any aspect of the cooling system. Communication in the other direction, however, namely from the process-control electronics to the detector subsystems, was possible in the form of interlocks that the cooling system could breach in the event of serious performance problems.

Each cooling platform was designed to maintain a specific, user-defined, fixed coolant-supply set-point temperature at approximately a constant flow rate of heat-transfer fluid, with an active feedback system that automatically compensated for changes in subsystem thermal power load, ambient temperature and humidity changes, and variations in heat-sink water temperatures and flow rates. Supply set-point temperatures were remotely selectable, and were designed to remain at most within ± 0.3 K of the requested temperature. All the farm platforms were designed to deliver flow rates up to approximately 23 L/min and to handle heat loads of up to approximately 1 kW. Table 1 provides a summary of the principal operating parameters of a generic CLEO coolant-control platform design; subsystem-specific requirements are described in Section 2.2 below.

2.2 Special subsystem requirements

Although the farm model was based upon identical platforms, some customization was nevertheless necessary to accommodate the specific needs of each of the new subsystems, described in Section 1, serviced by the coolant-control farm.

In the upgraded CLEO beam pipe, the thickness of beryllium separating the cooling channels from the inner accelerator vacuum volume and the outer atmosphere was 737 μm and 229 μm, respectively [6]. The differential pressure limit on the cooling-channel walls was therefore required not to exceed $\sim$203 kPa, necessitating the implementation of overpressure safeguards in the beampipe coolant-control platform (refer to Section 4).

Large pipe gauges in the plumbing leading to the drift-chamber cooling lines

Table 1
Summary of principal design parameters of a generic CLEO cooling platform.

Parameter	Type	Value
Coolant set-point temperature	minimum	287 K
	nominal	292 K
	maximum	299 K
Cooling capacity	maximum	1 kW
Flow rate, main circuit	maximum	23 L/min
Particulate impurity size	maximum	75 μm
Platform pressure	minimum	atmospheric
	maximum	690 kPa
Set-point temperature stability	minimum	$\pm$0.3 K
	maximum	$\pm$0.1 K
Subsystem pressure drop	maximum	$\sim$200 kPa

required a pump with a higher head rating to achieve adequate flow rates (refer to Section 4). The resultant increased flow capacity of the drift-chamber coolant-control platform allowed for this module to be used to provide temperature control to other passive devices (see Section 9). Due to the drift chamber's large size and mechanical sensitivity to uneven temperature distributions on the end plates, a dedicated interlock (described in Section 6) was required to prevent situations in which only a subset of the pre-amplifier electronics, mounted near the end plates, was powered while one set of global cooling parameters was applied to the entire heat-transfer area.

A similar motivation drove the customization in the control of heat-transfer fluid inside the RICH detector, for which there was a design necessity to be able to vary, in response to real-time conditions, the relative coolant flow rates through five azimuthally distinct regions of the detector. Rather than modify the RICH coolant-control platform itself, the main module was left generic and a separate "active-manifold" platform was designed to accommodate the furcation of a single global process-control loop into five individually controlled flow circuits. In Sections 4 and 5, aspects of the mechanical design and the special array of RICH coolant-temperature sensors required to construct and operate, respectively, the RICH active-manifold platform are discussed.

The upgraded silicon vertex detector was installed into the CLEO interaction region $\sim$4 months later in the commissioning period than the beam pipe, drift-chamber, and RICH subsystems; however, during this time, the silicon detector underwent electronics testing at a location $\sim$60 m remote from the CLEO experiment. The control system design therefore needed to be able to

provide uninterrupted interlock management and active coolant control of the installed systems while concurrently and flexibly supporting the testing of the silicon detector at the remote location.

3 Hydrocarbon heat-transfer fluids

The liquid coolant employed to remove heat from the detector subsystems consisted of PF^{TM}-200IG, an industrial solvent and degreaser manufactured by P-T Technologies, Inc. [9]. We know of no other applications that exploit the thermodynamic and flow characteristics of this substance in lieu of its chemical-contaminant solvency properties. Accordingly, we investigated several attributes of the PF^{TM}-200IG product, including its applicability to the cooling requirements of CLEO detector subsystems.

3.1 Coolant requirements

The hygroscopic nature of the cesium iodide in the CLEO barrel and endcap calorimeters [1] demanded that a heat-transfer fluid be employed in which CsI crystals were insoluble. Initially, the halocarbon compound 1,1,2-Trichloro-1,2,2-Trifluoroethane (Freon^{TM} [7] TF R-113 or Arcton^{TM} [8] 113) was used as a coolant, but its utility was limited by its ozone-depleting potential, its reactivity with beryllium, a propensity to leak without straightforward detection, cost, and a tendency to modify non-metal fittings such as ceramic pump seals, elastomers, and plastic sensor housings.

A second major consideration for a heat-transfer fluid to replace Freon^{TM} was therefore the requirement that it be compatible with the materials in each coolant circuit. In particular, this was a concern for the cooling channels in the thinly walled beryllium beam pipe, where corrosion avoidance was a necessity; Section 3.3 describes a study that addressed this compatibility.

In addition to the needed compatibility with CsI and Be, a suitable coolant was required to have thermodynamic and flow characteristics comparable to those of water. The heat-transfer fluid of choice was to be environmentally benign, be reasonably safe to handle, be non-corrosive to several different materials, and have preferably low electrical conductivity and negligible amounts of non-volatile residue remaining after evaporation. [9]

[7] "Freon^{TM}" is du Pont's registered trademark for its fluorocarbon compounds [10].
[8] "Arcton^{TM}" is a registered trademark of Imperial Chemical Industries Limited.
[9] In the event of a leak, high resistivity and complete evaporation were deemed necessary to minimize damage to electronics and detector components.

3.2 Properties of PF^{TM}-200IG

The substance PF$^{\mathrm{TM}}$-200IG is a non-flammable, electrically non-conductive, 100% volatile, aliphatic-hydrocarbon solvent with no ozone-depleting potential. It is a complex combination of normal paraffins (Alkanes) consisting of a straight chain of non-aromatic saturated hydrocarbons having carbon numbers in the range of C-5 through C-20 [11]. At ambient temperatures and pressures, PF$^{\mathrm{TM}}$-200IG is a colourless liquid that has a faint petroleum odour and is insoluble in water. The notation "200IG" identifies the product as of industrial grade, with a 200 °F (366 K) tag-closed-cup flash point.

Table 2 compares several properties of PF$^{\mathrm{TM}}$-200IG with liquid water and Freon$^{\mathrm{TM}}$ TF. We note that PF$^{\mathrm{TM}}$-200IG has $\sim$27% the thermal conductivity and $\sim$55% the specific heat capacity of water. Taking into account the lower density and higher kinematic viscosity (refer to Table 2), PF$^{\mathrm{TM}}$-200IG has approximately a factor of two worse heat-transfer capability as compared to water, for a given pumped plumbing circuit.

We studied the PF$^{\mathrm{TM}}$-200IG radiation length using 20 keV photons, finding it to be $\sim$52 cm ($\sim$44% longer than that for water). Particularly in the case of the beryllium beam pipe, where a cooling channel surrounded the vacuum chamber throughout the interaction region, the longer radiation length advantageously reduced the degradation of tracking resolution due to multiple scattering.

3.3 Compatibility of PF^{TM}-200IG with beryllium and other materials

The PF$^{\mathrm{TM}}$-200IG solvent was described by the manufacturer as non-corrosive to metals such as aluminium, copper, magnesium, and stainless steel [9]. Motivated by the type of metal used to construct the CLEO beam pipe, we undertook a study to examine the compatibility of PF$^{\mathrm{TM}}$-200IG with beryllium.

Three beryllium plates with dimensions 5.3 cm $\times$ 2.5 cm $\times$ 0.3 cm were each coated on one side with a corrosion resistant primer (BR127) and immersed in volumes of de-ionized water, PF$^{\mathrm{TM}}$-200IG, and air (the control sample), respectively. Following a period of 3 months at ambient temperature, pressure, and light exposure, there were no visibly discernible changes; the samples were subsequently placed near CESR where they absorbed a radiation dose of $\sim$25 krad.

With still no visually apparent deterioration in the exposed or primer-coated sides of the beryllium plates, we used a scanning electron microscope to examine the sample surfaces, micrographs of which are depicted in Figure 1. We

Table 2
Properties of PF^{TM}-200IG contrasted with those of liquid water and Freon^{TM}.

Property	PF^{TM}-200IG	Water	Freon^{TM} R-113	Units	Temp.
Auto-ignition temperature	483 [9]	–	–	[K]	–
Boiling-point temperature	466 – 516 [9]	373	321 [10]	[K]	–
CAS registry number	64771-72-8	7732-18-5	76-13-1	[–]	–
Chemical constitution	Paraffins, C5-20 [11]	H_2O	CCl_2F-$CClF_2$	[–]	–
Flash point	366 [9]	–	623 [10]	[K]	–
Heat of vapourization	247 [9]	2257 [12]	147 [10]	[kJ/kg]	boiling point
Kinematic viscosity	2.41 [9]	0.89 [12]	0.44 [10]	[cSt]	∼296 K
Radiation length	0.52	0.361 [13]	0.15 [13]	[m]	ambient
Specific gravity	0.79 [9]	1	1.56 [10]	[–]	ambient
Specific heat capacity	2303 [9]	4186 [12]	892 [10]	[J/kg·K]	∼292 K
Thermal conductivity	0.159	0.5984 [12]	0.074 [10]	[W/K·m]	∼294 K
Vapour pressure	0.041 [9]	6.75 [12]	62 [10]	[kPa]	311 K

observed that the sample that was in contact with PF^{TM}-200IG (Figure 1(c)) exhibited less surface modification than the sample that was in contact with H_2O (Figure 1(b)), as compared to the control sample (Figure 1(a)). Based on these observations, we concluded that PF^{TM}-200IG was at least as compatible with beryllium as de-ionized water.

In addition to our studies with beryllium, we tested the compatibility of PF^{TM}-200IG with other materials: cesium iodide, Buna and Viton^{TM} elastomers, Push-Lok® rubber hose, brass and stainless-steel fittings, copper, aluminium, plastic, and both polypropylene and nylon tubing. Our tests consisted of recording the masses and dimensions of the material samples and immersing them in containers of PF^{TM}-200IG under ambient conditions for a period of ∼8 weeks, whereupon we measured the mass changes and the frac-

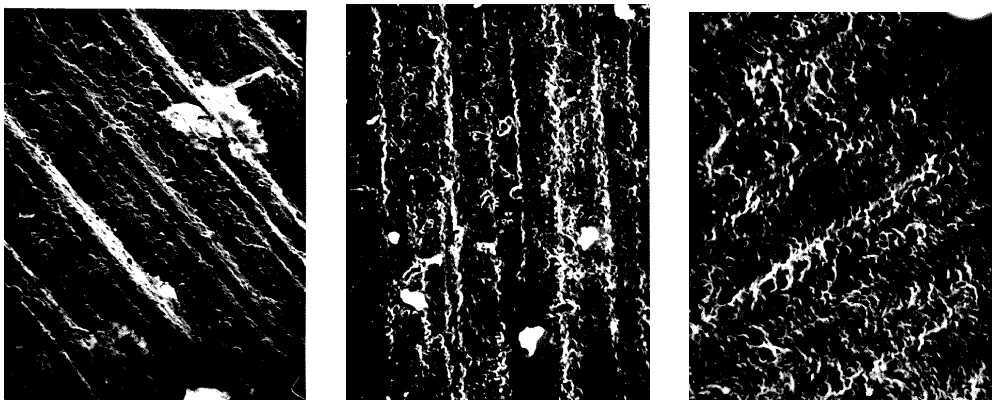

Fig. 1. Scanning electron micrographs of three beryllium surfaces (magnified ∼250 times) following contact with, from left to right, (a) air, (b) de-ionized H_2O, and (c) PF^{TM}-200IG after a period of over 3 months and a radiation dose of ∼25 krad. Note that all three samples show milling grooves with comparable periodicity.

tions of linear swell. For each of the materials tested, the observed changes in mass and size were negligible.

4 Mechanical construction

The mechanical design of the coolant-control platforms was driven primarily by the following criteria: reliability and serviceability; modularity; elevation and footprint; mobility; and ease of access to gauges, valves, filters, and reservoirs. The limited space in the "pit" beneath the CLEO detector, an approximately 16 m^2 area of ∼97 cm high crawl space, dictated a footprint of 76 cm × 76 cm and an elevation of ∼87 cm for each of the coolant-control platforms, including the RICH active-manifold platform. Each member of the farm was constructed on a rubber-footed skid of 0.6 cm thick aluminium, enabling a degree of mobility and easy access to platform facilities.

Figure 2 depicts a schematic of the coolant flow circuit on board one of the platforms in the farm. Upon leaving the reservoir due to suction from the pump, PF^{TM}-200IG coolant reached the pump inlet by way of either a branch through the hot side of a heat exchanger or via one of two bypass shunts. The cold side of the heat exchanger, the primary heat sink for the platform consisting of a 20-brazed-plate Cetetherm (Cetetherm AB, Ronneby, Sweden) honeycomb unit, was connected to a closed water circuit driven by a chiller system (refer to Figure 4). The amount of flow through the heat exchanger was regulated by a proportioning valve powered by a computer-controlled step motor; the fraction that the valve was open constituted the control variable in the feedback system. Unregulated 12 Vdc power supplies were mounted on each platform to power the proportioning-valve step motors.

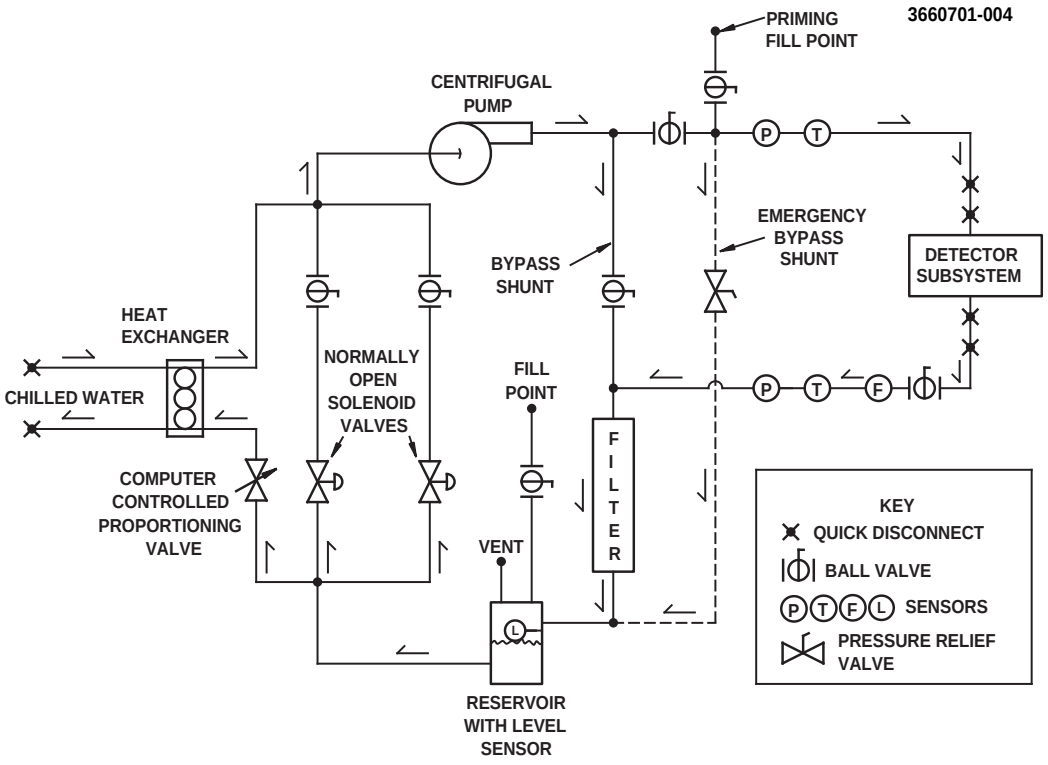

Fig. 2. Schematic of a hydrocarbon coolant circuit.

The two heat-exchanger shunt branches each contained a ball valve[10] and a normally-open solenoid valve. One design goal of the bypass system was to guarantee that there be flow to the detector subsystem at all times, assuming that both solenoid valves could never be simultaneously closed while the proportioning valve was 0% open. Dual bypass branches were implemented in order to expand the dynamic range of the system using binary flow logic. For a given fixed fractional flow rate in the bypass branches, large variations in the subsystem's heat load meant that the proportioning valve alone would not provide enough compensation to maintain a stable set-point temperature. Using solenoid valves to switch the two bypass branches, each with a fixed ball-valve setting, resulted in four discrete bypass flow configurations. With ball-valve settings appropriately chosen, the proportioning valve could provide full analog coverage for continuous flow changes intermediate to the four binary combinations of the two solenoid valves. We note that an alternative to this scheme to maximize the dynamic range would be simply to use a second proportioning valve in the heat-exchanger bypass shunt; we did not adopt this approach for reasons of reliability and economy.

Once through the outlet port of the pump, the PF^{TM}-200IG could either

[10] Ball valves were preferred over gate, globe, and needle valves because of their larger proportionality constants describing the achievable flow rates per unit of pressure drop at a given temperature.

bypass back through the filter and into the reservoir or depart the platform for transport to the detector subsystem, as indicated in Figure 2. The global rate of PF^{TM}-200IG flow leaving the platform was configured by partially closing the ball valve on the bypass branch leading back to the reservoir. Maximizing the fraction of flow through this bypass branch greatly assisted the feedback process by pre-cooling the temperature of the reservoir contents to near the set-point value.

The plumbing on the coolant-control platforms consisted primarily of brass 3/4" NPT threaded pipe fittings connected using approximately 79 nipples (sealed with Loctite PST® 567) per platform. Each platform also had ∼7 ball valves, ∼17 elbows, ∼6 couplings, ∼14 tees, and several bushings. Reservoirs were constructed from stainless steel, and the filter housings [11], also stainless steel, contained 75 μm polypropylene filters. The self-priming centrifugal pumps had stainless-steel casings, 750 W (2.2 kW for the drift-chamber platform) single-phase electric motors, and a 34 m (45 m for the drift-chamber platform) water head rating. Our determinations of these pump-head specifications took into account the flow requirements through the detector subsystems, the reduced density of PF^{TM}-200IG (refer to Table 2), the diameters and elevations of the plumbing runs, and the need for adequate flow in the bypass branches for optimum temperature control of the heat-transfer fluid. Throughout the plumbing of each platform, 12 stainless-steel unions were used to aid in the servicing of different components. An additional emergency bypass shunt containing a 690 kPa pressure relief valve linked the pump outlet port with the reservoir in the event of an overpressure situation. Refer to Figure 3 for an assembly drawing of a typical coolant-control platform.

At the maximum 23 L/min flow rates required by the design, the vapour pressure of PF^{TM}-200IG (refer to Table 2) was low enough to ensure that the cavitation number [12] was well in excess of the incipient cavitation value. No pressurization of the coolant circuits beyond ambient was therefore deemed necessary to avoid cavitation, permitting us to vent any of the reservoirs to the atmosphere during operation. In practice, we only vented the reservoir in the case of the beryllium beampipe cooling platform, where the differential pressure limit on the thin walls of the beryllium cooling channels was required not to exceed ∼203 kPa (refer to Section 2.2), a criterion that we also explicitly

[11] Our prototype platforms used polypropylene filter housings; although sprayed with conductive anti-static paint and fitted with ground straps, significant charge build-up due to the moving PF^{TM}-200IG dielectric separating the filter (also polypropylene) from the housing still resulted in some arcing. We therefore caution against the use of non-metallic housings and recommend that each coolant-control platform be carefully grounded.

[12] Cavitation number is a dimensionless quantity expressed as a quotient of the dynamic pressure, which is proportional to the density and the square of the flow rate, and the difference between the static and vapour pressures.

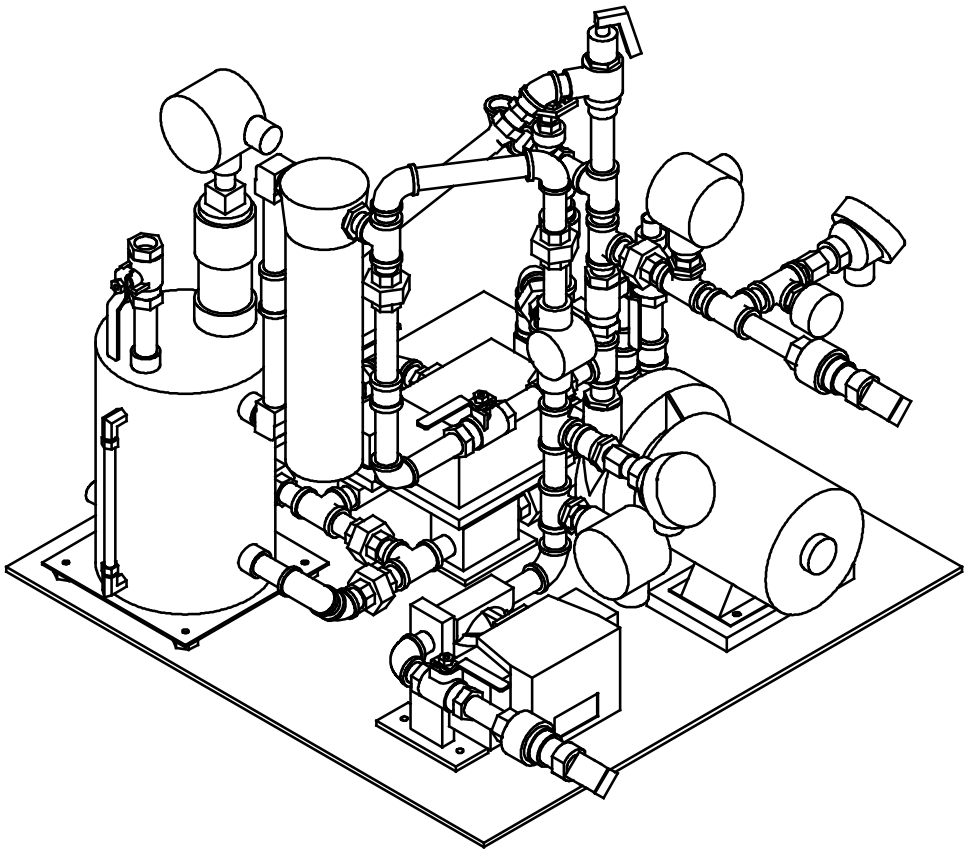

Fig. 3. Isometric assembly drawing of a coolant-control platform module, with the reservoir and the pump motor discernible in the left and right corners, respectively.

imposed on the system pressure near the outlet port of the pump on the platform proper. In lieu of the fixed (690 kPa) pressure relief valve, we installed an adjustable unit with the range $103 - 165$ kPa. As an extra precaution, the beampipe coolant-control platform also had a graphite rupture disc rated at 207 kPa. During prototype testing, we observed that this disc would rupture at what appeared to be lower than the rated pressure, as indicated by a glycerin-damped analog visual gauge. We ascribed this to transient pressure pulses from the pump's impeller and relief-valve oscillations; we subsequently installed a water-hammer suppressor in an effort to minimize the effect of these pulses.

Figure 4 depicts the main elements of the coolant-control farm, located in the pit beneath the CLEO detector, and the flow of cooling fluids (air, liquid water, and PF$^{\mathrm{TM}}$-200IG hydrocarbon) between them. Wherever possible, brass quick-disconnect fittings were used to link up the liquid connections, which were insulated with AP Armaflex$^{\mathrm{TM}}$. A closed-circuit water chiller system provided water near a temperature of 282 K to the cold sides of the heat exchangers residing on each of the coolant-control platforms (refer to Figure 2). In order to assist the water chillers, a heat exchanger to 280 K building water was inserted

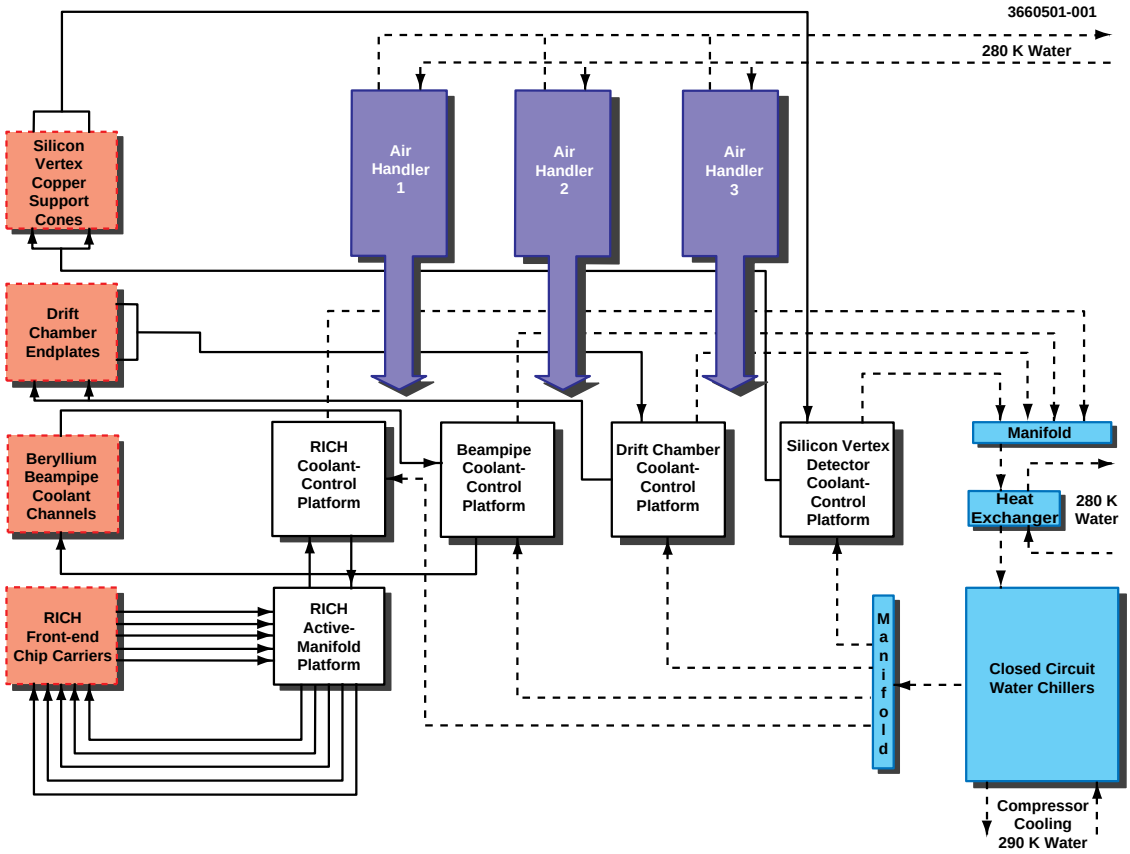

Fig. 4. Schematic layout of the CLEO coolant-control farm, showing flow circuits of the three cooling fluids: air (wide arrows), liquid water (dashed lines), and liquid hydrocarbon (solid lines, each representing an individually regulated circuit). The bifurcations in the supply and return lines to and from the silicon vertex detector and the drift chamber represent the division of coolant flow between the electron and positron sides of the CLEO detector.

to pre-cool the returning coolant. Three air handlers, their compressor coils cooled using 280 K building water, maintained a flow of cool dry air across the farm platforms. Also shown in Figure 4 is the RICH active-manifold platform, a dedicated module that consisted of two one-to-five manifolds, the supply manifold outfitted with five computer-controlled proportioning valves and the return manifold instrumented with five flow meters and transmitters.

5 Sensor elements

On or near the coolant-control platforms, the relatively harsh environment due to dust, water, hydrocarbons, EMI from pump and fan motors, and vibration demanded a design that made use of industrial sensor technologies. In order to minimize the amount of delicate electronics in the CLEO pit, the analog-

to-digital conversion of sensor signals took place in the control-system crate, described in Section 6. Standard industrial 4−20 mA transmitter technology was used to condition and send analog sensor signals from the farm platforms to the control system. Current transmitters had the advantages of greater noise immunity and an ability to send analog signals over relatively long distances. In addition, the remote sensors in the CLEO pit could be powered (usually using ∼3.5 mA of excitation current) and read out using a single shielded two-wire current loop, with no local power supply requirements. Because of the possibility for rigourous environmental conditions in the CLEO pit, all sensors in the design were required to have sealed weatherproof enclosures that fulfilled the specifications of the NEMA-4X standard.

As indicated in Figure 2, each coolant-control platform was instrumented with two temperature sensors, one supply and one return, to provide a measurement of the temperature rise due to the combination of subsystem power load, frictional heating of the moving coolant, and ambient heat transfer. The coolant supply temperature measurement was particularly critical since it served as the process variable in each of the main feedback control systems. This required the use of temperature sensors that were accurate and stable to less than ±0.1 K with low noise and good linearity characteristics. We investigated four temperature measurement technologies: thermocouples, resistance temperature detectors (RTDs), thermistors, and solid-state integrated circuits. Thermistors were too unreliable and nonlinear. We used solid-state devices, based on the AD592 (Analog Devices, Inc.) integrated circuit, in a prototype coolant-control platform, finding them to be attractive due to their relatively good linearity and well-defined characteristics, but difficult to insert into the coolant flow stream reliably and necessitating the design and production of a custom, weatherproof, diode-protected, 4−20 mA transmitter circuit (using, *e.g.*, the AD693 device). We concluded that the AD592 integrated-circuit sensors were better suited for measuring temperatures at the surfaces of solid objects rather than inside flowing fluids. We disfavoured a thermocouple solution because of the costs of the cold-junction compensation and linearization circuitry needed to achieve the desired accuracy. Our final design used tip-sensitive 100 Ω (industry standard IEC 751) platinum RTDs manufactured by Minco Products, Inc.; once combined with some relatively simple off-the-shelf linearization and 4−20 mA transmitter circuitry, RTDs were more linear, accurate, and sensitive than thermocouple implementations of comparable cost. A weatherproof 316 stainless-steel thermowell assembly safely housed the RTD and the front-end electronics, allowed for the effective insertion of the RTD directly into the flow of coolant, and permitted the replacement of the platinum element without having to breach the volume of heat-transfer fluid.

In addition to the pairs of temperature sensors instrumenting each of the farm platforms (as shown in Figure 2), the RICH system had a dedicated array of 32 tip-sensitive 100 Ω platinum RTDs distributed azimuthally and on both

the electron and positron sides of the detector in coolant-return manifolds located near the RICH modules. For these RTDs, 'hockey-puck' style 4−20 mA transmitters were mounted together in a single array located atop the CLEO detector; shielded wire leads, 18.3 m in length, connected the RTDs to these dedicated transmitters, which were calibrated to compensate for the net lead resistance. A custom-built multiplexer circuit facilitated addressed read-out of any one of the 32 temperature transmitters at a time.

Each coolant-control platform had visual pressure and flow-rate gauges to aid in manual adjustments to the flow configuration. In addition, every platform transmitted two pressure measurements, *i.e.*, the pressure drop through the CLEO subsystem and its plumbing network (refer to Figure 2), to the control crate using two 0−689 kPa Series 634E pressure sensors from Dwyer Instruments, Inc. Flow rates of heat-transfer fluid were transmitted from density-compensated vane-type flow sensors manufactured by Universal Flow Monitors, Inc. Level transmitters in the coolant reservoirs were manufactured by Omega Engineering, Inc., and consisted of a magnet that was mounted inside a stainless-steel float that tracked up and down an insertion stem while setting a series of reed switches in a voltage divider resistor network. The accuracies of the pressure, flow, and level sensors and transmitters used were ∼14 kPa, ∼1 L/min, and ∼1.3 cm, respectively.

6 Process-control system

The heart of the coolant-control system consisted of a small logic controller (SLC) module, a member of the SLC 500$^{\text{TM}}$ family of programmable controllers manufactured by Allen-Bradley Company, Inc., that resided in a dedicated 13-slot chassis with an integrated 1 A (24 Vdc) power supply module. The SLC 5/04 module used was capable of up to 4096 inputs plus 4096 outputs and had a memory of 32 K words. The remainder of the process-control system consisted of three other module varieties mounted in the chassis: a 32-channel current-sourcing digital DC output module (1746-OB32), three 4-channel 0−20 mA analog output modules (1746-NO4I) with 14-bit resolution, and eight 4-channel ±20 mA (±10 Vdc) analog input modules (1746-NI4) with 16-bit resolution.

The 13-slot Allen-Bradley chassis was mounted inside a crate enclosure positioned in the experimental hall outside the main radiation area. Also residing in the enclosure was a 24 Vdc/12 A regulated power supply used to energize the entire set of $4 - 20$ mA sensors remotely deployed both on the coolant farm platforms underneath the CLEO detector (refer to Figure 4), ∼35 m away, and in the array of 32 RICH temperature transmitters on top of the detector, ∼20 m away. Terminal blocks mounted on a DIN rail in the enclosure

served to interconnect the 24 Vdc power supply, the individual sensors, and the appropriate terminals of the analog input modules in the Allen-Bradley chassis. In the case of the 32 RICH transmitter signals, since the array was multiplexed, only a single analog input channel was required. The SLC clocked through the 32 addresses in 0.25 s intervals by using five of the digital output channels in the 1746-OB32 module to switch the 24 Vdc of the main sensor power supply.

The SLC processor used a ladder-logic programming language in which subroutines were organized into ladders, their rungs each acting as IF-THEN conditional statements. On the left side of every rung one or more conditions were defined; the corresponding right side executed one or more actions provided that all the conditions were met for the given rung. Editing of the ladder-logic code was achieved with RSLogix 500$^{\mathrm{TM}}$ (Rockwell Automation) programming software running on a networked Intel$^{\mathrm{TM}}$-based computer located in a clean computing environment and connected to the Allen-Bradley control crate by a 30 m RS-232 serial connection. The ladder-logic code was compiled with the RSLogix 500$^{\mathrm{TM}}$ software and was communicated to the SLC 5/04 module using a dedicated utility (RSLinx$^{\mathrm{TM}}$). In a similar manner, this serial communication configuration had the capability to allow online edits, parameter adjustments, and diagnostic readout of inputs, outputs, and internal memory structures *during* programme execution in the SLC.

The Allen-Bradley SLC control code consisted of $\sim$260 rungs organized into a main ladder that cycled through a series of calls to 14 subroutine ladders. For each of the beampipe, drift-chamber, RICH, and silicon subsystems there were subroutines for platform sensor data acquisition, interlock decisions and output, and process control. The RICH system had two extra subroutines, one to read out the multiplexed RICH temperature signals and one to perform process-control duties and flow-sensor data acquisition for the RICH active-manifold platform.

During every cycle of control code execution, an interlock decision was taken for each of the farm platforms. The four criteria forming this decision consisted of a minimum coolant flow rate, minimum and maximum set-point temperatures, and a minimum level of heat-transfer fluid in the reservoir (for leak detection). Supply and return pressure criteria were not included in the interlock decisions. For a given farm platform, if these conditions were all satisfied, the interlock ladder logic would use a channel in the 1746-OB32 output module to energize a normally open relay switch mounted to the DIN rail near the terminal blocks in the chassis enclosure. The cooling-interlock relays were connected to a higher-level interlock crate that could switch off power to the subsystem electronics crates in the event of a failure. The control system was designed such that there would also be an interlock breach if the Allen-Bradley SLC had any interruption in power.

Specific to the drift-chamber coolant-control platform, an additional interlock was used to reduce the possibility of cooling the chamber end plates unevenly, a situation that potentially posed deleterious consequences to the chamber's mechanical integrity. If part or all of the drift-chamber electronics underwent an unexpected loss of power, the power to the centrifugal pump on the coolant-control platform was switched off by means of a relay on a 10-minute delay. In turn, this would render the minimum-flow-rate criterion unsatisfied, thereby breaking the cooling interlock and removing power from all of the drift-chamber electronics crates.

At the core of the process-control logic in each closed feedback loop was a proportional integral derivative, or PID, instruction tuned to maintain a desired setting of an input process variable by computing appropriate real-time adjustments to an output control variable. For each coolant-control platform, the process variable consisted of an input from the platinum RTD sensor measuring the temperature of the heat-transfer fluid supplied to the detector subsystem; the control variable consisted of the fractional opening of the heat-exchanger proportioning valve, as set by the step motor positioned using $4-20$ mA signals from the 1746-NO4I analog output modules (refer to Figure 2). In order to increase step-motor life, a deadband of 0.1 K was used in the PID algorithm; in this way, the control variable was left unchanged once the process variable passed through the set point and until it was different from the set point by the deadband amount.

7 Diagnostic system

For reasons of reliability and flexibility, the diagnostic and process-control systems for the CLEO coolant-control farm were kept relatively independent through the use of a two-tiered configuration. Notwithstanding, the same networked computer that was used to upload the compiled ladder-logic code into the Allen-Bradley SLC, as described in Section 6, served as the run-time implementation platform for the diagnostic software.

A graphical programming language was used to develop a user interface, also graphical, to the diagnostic system parameters. The software was based on virtual instruments (VIs) in the LabVIEW$^{\text{TM}}$ environment provided by National Instruments Corporation. During normal farm operation, *i.e.*, when the SLC was in a 'standalone' mode and assumed sole control of the farm, the RS-232 serial connection between the SLC and the networked computer (refer to Section 6) could be used by the LabVIEW$^{\text{TM}}$ software to read out regions of the SLC memory for diagnostic purposes. Code from proprietary driver and VI libraries (HighwayVIEW$^{\text{TM}}$, from SEG, Watertown MA, USA) transacted the data between the SLC and the LabVIEW$^{\text{TM}}$ software.

Although the diagnostic interface primarily read data from the SLC for the purpose of displaying them to users, it did provide password-privileged cooling experts with the ability to adjust the platform set-point temperatures maintained by the control system. Such set-point changes were effected, again using a HighwayVIEW^{TM} VI, by writing data into SLC memory via the serial interface. Users of the local area network could therefore "window in" to the LabVIEW^{TM} computer to view real-time diagnostics and, if necessary, make limited adjustments to the control parameters.

Diagnostic information was made available to other subsystem experts and data-acquisition personnel by hypertext transfer-protocol (http) servers running on the LabVIEW^{TM} computer. For each platform in the farm, there was an http server capable of delivering streaming quasi-real-time images of the main LabVIEW^{TM} front panel to a client web browser. An example of one of these web-based front-panel displays is given in Figure 5. Other web accessible displays included special diagnostics for the RICH temperature-sensor array (Section 5), RICH active-manifold parameters (Section 4), and virtual strip charts giving a graphical representation of the 12-hour history of some of the more important system parameters.

In addition, every minute, the LabVIEW^{TM} machinery updated a detailed text-only html file containing an expert diagnostics digest that listed the status of all farm parameters. This diagnostic file was written to public web space and was accessible remotely using the WWW. In particular, the digest file format lent itself well to remote small-screened portable devices like personal digital assistants using mobile infrastructure software such as that available from AvantGo, Inc. Long-term archiving of the coolant-control farm operating history was achieved by taking half-hourly snapshots of the expert diagnostics digest file, compressing them, and storing them in a database.

8 System performance

Maintenance of the farm platforms proved to be minimal, consisting of weekly visual inspections and annual cleanings and polypropylene filter replacements. Some minor coolant leaks, requiring occasional top ups, were detected by the observation of changes in reservoir level readings with time. In the beampipe and silicon-detector systems, which each had longer runs of Push-Lok® rubber hose connecting the platforms to the subsystems, the PF^{TM}-200IG acquired an orange colour, contrary to earlier compatibility studies (refer to Section 3.3). We attributed this discolouration to the dissolution of a powdered protectant with which the inner surfaces of the Push-Lok® rubber had been treated; although no degradation of the hose was observed, we recommend using polypropylene or nylon tubing in future applications.

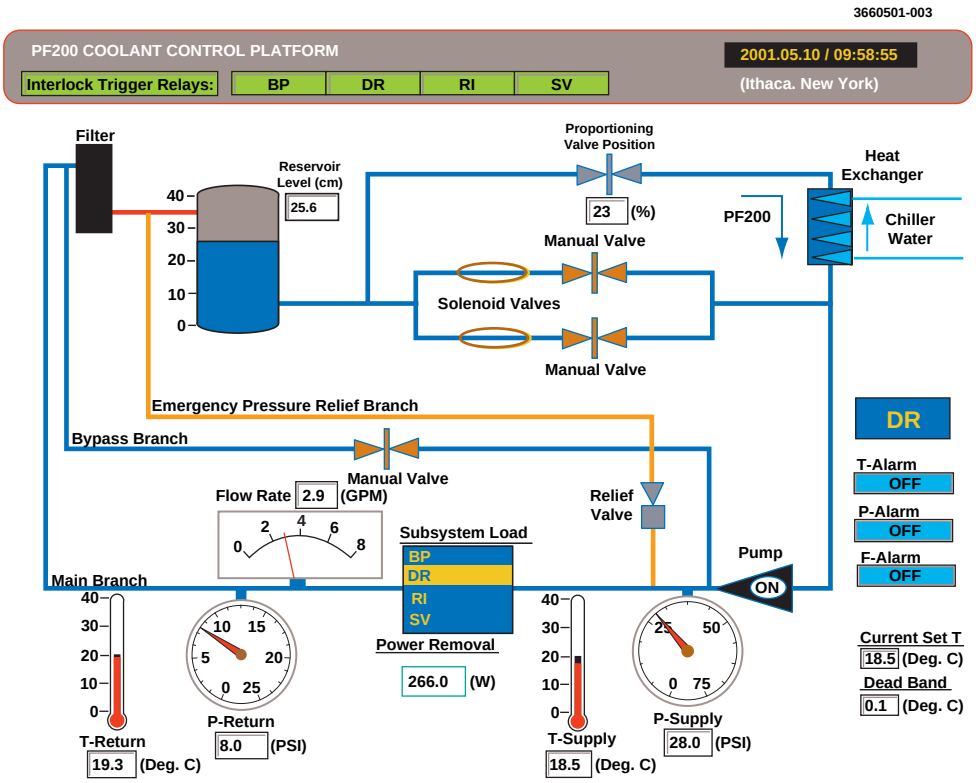

Fig. 5. Web-based diagnostic panel for real-time viewing of the principal performance parameters of a given coolant-control platform, in this example that for the drift-chamber (DR) detector subsystem. Similar displays describe the other subsystems. This image was recorded during the CLEO III datataking run.

Operationally, the dynamic ranges of the proportioning valves alone precluded a need to switch the solenoids in the heat-exchanger bypass shunts in order to maintain PID control. With fixed ball-valve openings in the two shunt branches and a deadband setting of ± 0.1 K in all the PID loops, supply temperatures were asserted with a stability of ± 0.2 K with respect to the set-point values for the duration of the CLEO III datataking period. This degree of control was exploited during CLEO III commissioning in pedestal sensitivity studies of the CLEO beampipe PIN-diode radiation monitors [14], for which the beampipe coolant-control platform was employed to vary the coolant supply temperature between 293 K and 299 K.

The CLEO coolant-control farm commenced operation in November 1999 with the beginning of the CLEO III commissioning period. As described in Section 2.2, prior to March 2000 the silicon farm platform was deployed remotely and was successfully operated and monitored by the central farm control and diagnostics systems, respectively. On 16 March 2000, a building cooling-water

pipe burst, flooding the CLEO pit and submerging the farm platforms under ∼25 cm of water; all sensors, power supplies, and pumps, after drying and cleaning, survived the event. On a few other occasions, many of the farm's interlocks were exercised in power failures or due to temperature variations in the 290 K water supply that caused trips in the chiller compressors (refer to Figure 4). The Allen-Bradley SLC 5/04 module (described in Section 6), which was equipped with a battery back-up system, was rendered immune to brief power glitches and, it was found, could be relied upon as though it were a firmware device.

The CLEO III detector began taking physics quality data in July 2000 for a run that ended in June 2001, with a scheduled three-week down in September 2000. The coolant-control farm induced no CLEO or CESR downtime in this period, during which a time-integrated luminosity of ∼9 fb^{-1} was accumulated.

9 Conclusions and outlook

We have described a novel approach to active particle-detector cooling that is based upon a farm of modular coolant-control platforms charged with the hydrocarbon solvent PF$^{\text{TM}}$-200IG, uniquely used as a heat-transfer fluid [9]. During the CLEO III datataking run, the farm provided reliable cooling support to the RICH detector, the drift chamber, the silicon vertex detector, and the beryllium beam pipe, with a temperature stability that exceeded design specifications.

The CLEO hydrocarbon coolant farm will see continued service in an upcoming programme of operation to explore the Υ resonances, charm physics, and quantum chromodynamics (CESR-c/CLEO-c) [15]. As mentioned in Section 2.2, the drift-chamber platform, by virtue of its greater flow capacity, is being upgraded to provide additional cooling for passive permanent-magnet (NdFeB) quadrupole elements [16] that are being installed prior to the Υ resonance running period. Other aspects of the farm will remain the same.

We have shown that a centrally controlled and monitored farm of generic active coolant-control platforms, running the liquid hydrocarbon solvent PF$^{\text{TM}}$-200IG as a heat-transfer fluid, can provide independent and regulated heat removal from several different subsystems in a particle-physics detector. Aspects of this design are applicable to future high-energy physics apparatus where flexibility, minimal maintenance, and the ability to monitor and operate detector and accelerator systems remotely will be progressively important.

Acknowledgements

We would like to thank K. Powers and G. Trutt of the Wilson Synchrotron Laboratory, Cornell University, for their excellent technical support. This work was supported by the U.S. National Science Foundation, the U.S. Department of Energy, and the Natural Sciences and Engineering Research Council of Canada.

References

[1] Y. Kubota *et al.*, Nucl. Instr. and Meth. A **320** (1992) 66.

[2] T.S. Hill, Nucl. Instr. and Meth. A **418** (1998) 32.

[3] M. Artuso *et al.*, Nucl. Instr. and Meth. A **441** (2000) 374, [hep-ex/9910054].

[4] D. Peterson *et al.*, Nucl. Instr. and Meth. A **478** (2002) 142.

[5] J. Fast *et al.*, Nucl. Instr. and Meth. A **435** (1999) 9.

[6] S. Henderson and S. Roberts, Proc. Part. Acc. Conf. **2** (1999) 1351.

[7] E. Nygard *et al.*, Nucl. Instr. and Meth. A **301** (1991) 506.

[8] E. von Toerne *et al.*, Nucl. Instr. and Meth. A **473** (2001) 17.

[9] P-T Technologies, a division of LPS Laboratories, 4647 Hugh Howell Rd., P. O. Box 105052, Tucker, Georgia 30085-5052, USA; Material Safety Data Sheet and private communication. Note that the substance PF$^{\rm TM}$-200IG is a discontinued product; possible replacement heat-transfer fluids are being considered, including PF$^{\rm TM}$-145HP, also manufactured by P-T Technologies.

[10] E.I. du Pont de Nemours and Company, Inc., Wilmington, Delaware 19898, USA; International Chemical Safety Card #0050.

[11] *CHEMLIST* Database, Copyright 2001 ACS (accessed 26 April 2001 using *SciFinder Scholar*).

[12] CRC Handbook of Chemistry and Physics, 81st Edition, editor-in-chief D.R. Lide, CRC Press, Boca Raton, 2000.

[13] D.E. Groom *et al.*, Eur. Phys. J. C **15** (2000) 1.

[14] M. Dubrovin and D. Cinabro, Cornell Internal Notes No. CBN 00/7 and CBX 00/28, 2000 (unpublished).

[15] CLEO Collaboration, CLEO-c and CESR-c Taskforce, "CLEO-c and CESR-c: A New Frontier of Weak and Strong Interactions", Cornell Report No. CLNS 01/1742, 2001 (unpublished); L.K. Gibbons, [hep-ex/0107079].

[16] W. Lou, D. Hartill, D. Rice, D. Rubin, and J. Welch, Phys. Rev. ST Accel. Beams **1** (1998) 022401.